Conclusion: The dosimeter's deformable properties are not altered significantly by repeated strain or irradiation, its volume is conserved under compression and it displays predictable behavior when being irradiated under strain. These properties makes the dosimeter a very strong candidate for direct dose measurement in deformed geometries.

PO-0830

Correlation of MLC positions detected using log-files with MLC positions detected using the EPID

W. Lechner[1,2], A. Moser[1,2], A. Altendorfer[1,2], D. Georg[1,2]
[1]*Medical University of Vienna, Department of Radiation Oncology, Vienna, Austria*
[2]*Medical University of Vienna, Christian Doppler Laboratory for Medical Radiation Research for Radiation Oncology, Vienna, Austria*

Purpose or Objective: The Purpose of this work was to investigate the long term correlation between leaf positioning errors determined using LINAC log-files with an independent method.

Material and Methods: A picket fence pattern was irradiated on four different LINACs with simultaneous EPID measurement and log-file recording. Measurements were performed on two VersaHD and two Synergy LINACs (Elekta AB, Stockholm, Sweden) over a period of six months on a weekly basis. The picket fence pattern consisted of 5 bands with a width of 2 cm. The positions of bands' centers were -11 cm,-2 cm, 0 cm, 2 cm and 11cm. An in-house developed software was employed to calculate the deviation of the actual leaf positions according to the log-file data from the planned position. The simultaneously acquired EPID images were analyzed using MLCSoft-EPID (PTW, Freiburg, Germany) and provided reference data. The sensitivity of all measurement methods was evaluated by means of implementing leaf errors in the picket fence pattern. The sensitivity of both methods was investigated by artificially introducing leaf positioning errors of 0.5 mm, 1 mm and 2 mm. In order to investigate the correlation between log-file and EPID data, Pearson's correlation coefficient was calculated considering all leafs as unity of each LINAC over the measurement period (henceforth denoted as total correlation coefficient ptot). Additionally, Pearson's correlation coefficient was calculated for each leaf separately (pL). The percentage of the absolute value of pL exceeding 0.6 was reported.

Results: The artificially introduced errors were detected by both measurement systems. The total correlation coefficients for LINAC 1, LINAC 2, LINAC 3 and LINAC 4 were 0.44, 0.06, 0.61 and -0.19, respectively. In contrast to that, only 0%, 2.04%, 6% and 0% of the absolute values of correlation coefficients calculated for each leaf separately exceeded a value of 0.6. These results are summarized in Table 1. In Figure 2 depicts an example of a scatter plot of the data acquired for LINAC 2.

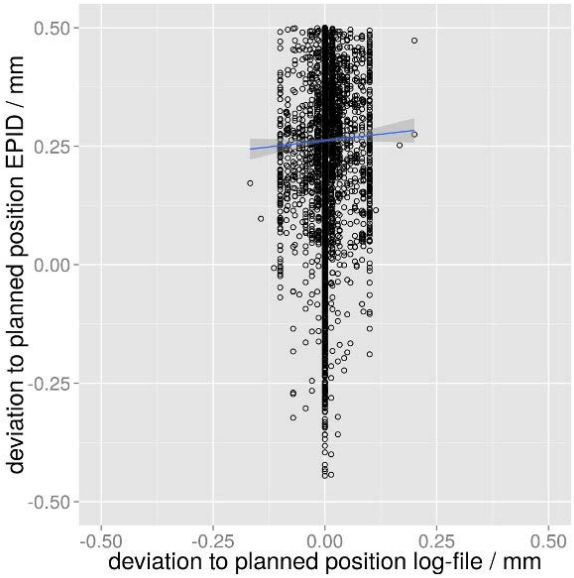

Fig 1: Scatter plot of all simultaneously measured leaf deviations of LINAC 2. The blue line represents a linear fit of the data. The correlation coefficient for this LINAC was 0.06

Table 1:

	LINAC 1 Synergy	LINAC 2 VersaHD	LINAC 3 Synergy	LINAC 4 VersaHD
p_{tot}	0.44	0.06	0.61	-0.19
abs(p_L) > 0.6 (%)	0	2.04	6	0

Conclusion: When investigating the correlation of MLC positioning errors detected with different methods, it is not sufficient to consider correlation coefficients based on sets of leafs, since a bias could be introduced. Such correlations must be investigated for each single leaf separately. This investigation revealed a poor correlation between log-file detected leaf positioning errors with EPID detected leaf positioning errors. However, deviations from planned leaf positions can potentially be detected using log-files, provided that a rigorous MLC quality assurance procedure using an independent system is performed on a regular basis.

PO-0831

Does a single MLC characterization guarantee a high accuracy of RapidArc delivered dose?

A. Scaggion[1], N. Pivato[1], A. Roggio[1], M. Paiusco[1]
[1]*Insituto Oncologico Veneto IOV-IRCCS, Medical Physics, Padova, Italy*

Purpose or Objective: In order to improve the accuracy of RapidArc delivered doses, users of Eclipse TPS commonly are forced to tailor the values of dosimetric leaf gap (DLG) and MLC transmission factor (TF). The aim of this work is to propose a methodology to improve the agreement between planned and delivered dose identifying a suitable group of (DLG,TF) couples.

Material and Methods: The 2D variation of DLG and TF has been measured for a Varian Unique Linac equipped with a Millennium 120 MLC. Using the 2D maps of DLG and TF an optimal couple (DLG,TF) has been computed for 50 treatment plans including H&N, chest and pelvis. A clinical couple (DLG,TF) has been computed as the mean over each optimal couple for the entire group of plans and for subgroups. Pre-treatment QA has been performed using a cylindrical diodes array and analyzed using both gamma index and DVH-oriented metric. QA results of any calculated plan has been correlated with the distance between the clinical couple and the optimal one. Finally a sensitivity analysis has been performed to assess a relation between the results of pre-

treatment QA and the minimum number of clinical couples (DLG,TF) needed to ensure the acceptance of all plans.

Results: The optimal couple of (DLG,TF) was found to vary with MLC motion complexity: as the MLC apertures became smaller and more irregular DLG and TF increase. As a consequence the optimal value of (DLG,TF) vary with district from (2mm,1.7%) for prostate plans to (2.35mm,1.9%) for H&N ones. Despite this rough classification, some differences within the same district can arise when target volumes are significantly different from typical values.Because of this differences the use of a single couple (DLG,TF) can lead to mean dose deviations as large as 5% between planned and delivered dose. In our case three different (DLG,TF) couples were found to be enough to ensure a local gamma (3%,3mm) passing rate larger than 95% for each plan.Once a significant database has been collected the optimal couple (DLG,TF) to be used for a new plan can be a priori decided considering the anatomical district. The choice can be then confirmed after a single optimization process computing the optimal couple for that plan and evaluating the distance from the clinical couple to foresee the expected degree of dosimetric agreement.

Conclusion: Our work shows that a single optimal couple (DLG,TF) can not be found for all possible clinical plans, but three MLC configurations can be enough to ensure the accuracy of delivered dose. A method to identify the group of MLC configurations is proposed together with indications about how to identify the appropriate couple to be used for any plan.

PO-0832

Preliminary scanning water phantom data for beam characterisation of a hybrid MRI-Linac

S. Woodings[1], H. Van Zijp[1], T. Van Soest[1], P. Woodhead[2], M. Duglio[2], N. Marinos[2], S. Pencea[2], D.A. Roberts[2], J. Kok[1], J.W.H. Wolthaus[1], B.W. Raaymakers[1]
[1]*University Medical Center Utrecht, Radiotherapy, Utrecht, The Netherlands*
[2]*Elekta Limited, Linac House, Crawley, United Kingdom*

Purpose or Objective: An Elekta MR-Linac (MRL) prototype has been installed at the author's institute, combining 1.5 T magnetic resonance imaging (Philips) with linear accelerator treatment (Elekta). A novel method for alignment and use of a scanning water phantom has been established. The first data of sufficient precision and quantity to characterize the beam has been acquired in a 1.5 T magnetic field for the purposes of beam modelling and/or beam verification.

Material and Methods: The isocentre is located at 143.5 cm from the linac target and is within an enclosed MRI-like bore which affects the use of a water phantom. A prototype MR-compatible water phantom (PTW) was used to acquire percentage depth doses, inline and crossline scans, relative output factors and collimator scatter factors with a CC04 ion chamber (IBA) and a micro-diamond detector (PTW). An exit PDD showing the electron return effect was also acquired. Position and orientation of the phantom was established using radio-opaque markers and a gantry-mounted electronic portal imaging device.
Linac-specific parameters such as gantry tilt, EPID rotation and isocentre location were independently checked using the water phantom.

Results: The beam energy is consistent with a nominal 7.3 MV photon beam (TPR 0.702), however the depth of maximum dose is 13 mm, closer to the surface than in a standard field due to the 1.5 T magnetic field. Inline profiles are generally consistent with those of a standard flattening-filter-free beam, however the crossline profiles are clearly distinct with an off-axis shift and asymmetric penumbral shoulders and feet due to the Lorentz force of the magnetic field on the secondary electrons. Small field data were acquired taking into account the dose-shift due to the magnetic field. The relative output factors are consistent with those from a standard FFF beam, with no evidence of abnormal variation for small fields.
Final results will be presented.

Conclusion: Practical use of a scanning water tank has been established in an MRL. The data presented here comprises the first substantial collection of MRL data that can be used for beam characterization. The dataset is suitable for calculating relative doses and testing planning system model performance in a 1.5 T magnetic field.

Poster: Physics track: Radiation protection, secondary tumour induction and low dose (incl. imaging)

PO-0833

Measured neutron spectra & dose: craniospinal irradiation on single-room passively scattered proton

R. Howell[1], E.A. Burgett[2], D. Isaccs[2], S.G. Price Hedrick[3], M.P. Reilly[3], L.J. Rankine[3], K.K. Grantham[3], S. Perkins[3], E.E. Klein[3]
[1]*UT MD Anderson Cancer Center Radiation Physics, Radiation Physics, Houston- TX, USA*
[2]*Idaho State University, Nuclear Engineering, Pocatello, USA*
[3]*Washington University, Radiation Oncology, St. Louis, USA*

Purpose or Objective: Secondary neutron dose is of particular concern in proton craniospinal irradiation (CSI) as this treatment is primarily used to treat children and adolescents, who are at significant risk of developing radiation-related late effects. While Monte Carlo techniques have been used to calculate such data for proton CSI, doses that are based on spectra measurements are lacking in the literature. Furthermore, the existing data are only reported for one of the proton beamline manufacturers. Given that doses from externally generated neutrons are highly dependent on the design of the proton therapy machine itself and treatment-specific devices within the beamline, there is a need to report doses for all beamlines used to treat proton CSI. Single-room compact proton systems are particularly noteworthy as many units are currently operational and more are being commissioned and installed. Therefore, the objectives of the present study, for a typical passively scattered proton CSI treatment, were to measure the secondary neutron spectra and calculate dose equivalents for neutrons delivered via a single-room compact system.

Material and Methods: Secondary neutron spectra were measured using extended-range Bonner spheres for three different clinical CSI proton fields, including their respective brass apertures: whole brain, upper spine, and lower spine. For each field, measurements were repeated with an active scintillator and 18 different moderating. Measurements were performed with a water phantom at isocenter and the detector located at 50 cm from the isocenter along the patient plane. For each set of measurements, neutron spectra were determined by mathematical deconvolution of detector count rates. Ambient dose equivalents [H*(10)] were calculated using ICRP-74 conversion coefficients to the fluence spectra.

Results: The measured neutron spectral fluence and H*(10) for each field are shown in Figure 1a and 1b, respectively. The energy distributions for each of the fluence spectra were similar, with a high-energy direct neutron peak, an evaporation peak, a thermal peak, and an intermediate continuum between the evaporation and thermal peaks. Neutrons in the evaporation peak made the largest contribution to the dose equivalent. The, H*(10) in mSv per proton Gy to isocenter were 3.94, 2.79, and 2.71 respectively, for the brain, upper spine, and lower spine fields. Neutron fluence and H*(10) were approximately 1.6 times higher for the brain field than for the spine fields, which is attributed to the greater range and modulation for the brain field than for the spine fields.